Available online at www.sciencedirect.com
ScienceDirect
Chemical Physics Letters 443 (2007) 328–332
CHEMICAL PHYSICS LETTERS
www.elsevier.com/locate/cplett

Finite length effects in DNA-wrapped carbon nanotubes

S.G. Chou [a,1], H. Son [b], M. Zheng [c], R. Saito [d], A. Jorio [e], G. Dresselhaus [f], M.S. Dresselhaus [b,g,*]

[a] Department of Chemistry, Massachusetts Institute of Technology, Cambridge, MA 02139-4307, United States
[b] Department of Electrical Engineering and Computer Science, Massachusetts Institute of Technology, Cambridge, MA 02139-4307, United States
[c] DuPont Central Research and Development, Experimental Station, Wilmington, DE 19880, United States
[d] Department of Physics, Tohoku University and CREST JST, Aoba, Sendai 980-8578, Japan
[e] Depto. de Física, Universidade Federal de Minas Gerais, Belo Horizonte-MG 30123-970, Brazil
[f] Francis Bitter Magnet Laboratory, Massachusetts Institute of Technology, Cambridge, MA 02139-4307, United States
[g] Department of Physics, Massachusetts Institute of Technology, Cambridge, MA 02139-4307, United States

Received 24 April 2007; in final form 18 June 2007
Available online 23 June 2007

Abstract

Resonance Raman studies have been carried out on length-sorted single walled carbon nanotubes (SWNTs). For nanotubes much shorter than the wavelength of light, a large increase in Raman intensity is observed for several features in the intermediate frequency mode (IFM) region. The changes in IFM intensities are found to be highly dependent on the laser excitation energies, the (n,m) indices, and the specific Raman features. A direct correlation is found between the amount of IFM intensity increase as a function of the average nanotube length, as well as the symmetry of the physical origin for the specific IFM feature.

1. Introduction

Length separation of single walled nanotubes (SWNTs) has been one of the on-going themes in nanotube research. The availability of SWNT samples with precisely controlled geometry not only facilitates device engineering, but the availability of SWNT samples with average lengths much shorter than the wavelength of light also allows one to study the finite length effects associated with the broken translation symmetry along the axial direction of SWNTs.

Extensive theoretical studies have been carried out to understand finite length effects on the electronic and optical properties of SWNTs [1–3]. In particular, the vibrational structures in the intermediate frequency mode (IFM) region between 600 cm^{-1} and 1500 cm^{-1} have been of special interest, since the finite length effects associated with the broken translational symmetry along the axial direction increase the ordinarily low Raman cross section for the IFM features and give rise to larger spectral intensity, which is beneficial to their systematic study. Many previous resonance Raman studies have investigated the weak IFM features (between the radial breathing modes and the G-band region) and their detailed (n,m) dependence [1–6]. Fantini et al. [5] have explained the origin of the IFM features, as well as their very special excitation energy, E_{laser}, dependence, on the basis of resonance processes in the 1D SWNT system associated with the combination of zone-folded optical and acoustic branches from 2D graphite. Further Raman studies have extended the model to relate the detailed spectral dispersion behavior to different SWNT diameters, metallicity (whether the nanotube is metallic or semiconducting), and resonant E_{ii} transitions [6]. On the other hand, no systematic study has yet been carried out to explore the theoretically predicted IFM intensity dependence on nanotube length (L_{tube}).

* Corresponding author. Address: Department of Electrical Engineering and Computer Science and Department of Physics, Massachusetts Institute of Technology, Cambridge, MA 02139-4307, United States. Fax: +1 617 253 6827.
E-mail address: millie@mgm.mit.edu (M.S. Dresselhaus).
[1] Present address: Pfizer Global Research and Development, Groton, CT 06340, United States.

0009-2614/$ - see front matter © 2007 Published by Elsevier B.V.
doi:10.1016/j.cplett.2007.06.091

Recent developments in the size exclusion chromatography (SEC) technique [7–10] have enabled the length separation of DNA-wrapped SWNTs. In this study, a systematic resonance Raman study is carried out on DNA-wrapped SWNT samples with controlled average tube lengths to study the effects of broken translational symmetry in short SWNTs. As the average L_{tube} decreases, many of the IFM features are found to show an increased Raman cross section as a result of reduced translational symmetry. The increase in the Raman intensity is found to be highly dependent on the symmetry for the physical origin of the IFM feature. The dependence of the D-band intensity on the inverse L_{tube} has been previously studied in these samples[11], and this dependence was closely related to more general studies of the D-band intensity dependence on crystalline size [12].

In addition, the increased contribution of the end-cap in short nanotubes also yields enhanced intensities for several vibrational features associated with fullerenes. The present study provides direct experimental evidence for the increased Raman cross section of IFM Raman features in short nanotubes, as previously predicted [1,2]. The different behavior of the IFM intensities (I_{IFM}) with respect to L_{tube} also provides new insights into the intrinsic physical processes that give rise to the IFM features.

2. Experimental

Three samples of DNA-wrapped CoMoCAT SWNTs with average L_{tube} of 50 nm, 70 nm, and 100 nm were prepared, following procedures established in previous reports [7–10]. The average length for each of the fractions has been estimated to be about 10% [7]. The samples used for optical characterization were prepared from the fractionated liquid samples by dropping 15 μL of the same stock solution onto a piece of sapphire substrate, 1 μL at a time. The resonance Raman measurements were carried out using a home-built micro-Raman system through a 50× microscope objective in the backscattering geometry. The spectra taken at the same laser excitation energy are later normalized with respect to their G-band intensities. The laser excitation energies were generated from a Kr^+ ion laser and a dye laser. A thermoelectrically-cooled Si CCD detector was used in conjunction with both lasers. The laser power level on the sample was kept below 0.45 mW to prevent overheating the sample.

3. Results and discussion

The DNA-wrapped, as-grown CoMoCAT SWNT sample (called the as-grown sample to indicate CoMoCAT tubes for which no length sorting had occurred) was used as a standard to differentiate the effects of length sorting. Since these samples have not been treated with the SEC (size exclusion chromatography) separation technique, the spectra for the standard represent an ensemble average of different values of L_{tube}, most of which are more than several hundred nanometers in length. For the first experiment, the laser excitation energy, E_{laser}, was chosen at 647 nm (1.92 eV) because this energy is highly in resonance with the lowest excitonic transition for the (7,5) SWNT. All four spectra shown in Fig. 1a are normalized with respect to their G-band intensities, and only one dominant radial breathing mode (RBM) associated with the (7,5) SWNTs could be observed for all of the samples. This particular choice of E_{laser} allows one to focus on the effects of nanotube length (instead of diameter and chirality) on the Raman spectra.

The spectral features associated with the 100 nm length sample closely resemble the features of the as-grown sample, in which the average nanotube lengths, are estimated to be at least several hundred nanometers. As L_{tube} decreases, more IFM features can be identified in the

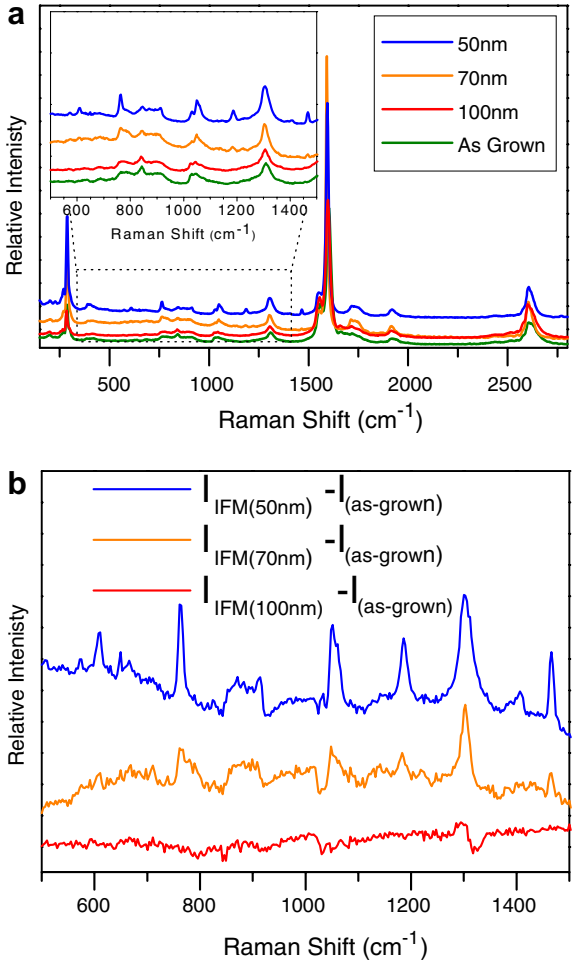

Fig. 1. (a) A comparison of the resonance Raman spectra for four SWNT samples, including an ensemble of as-grown DNA-wrapped SWNTs and three SEC-treated SWNT samples with L_{tube} of 50 nm, 70 nm, and 100 nm [6–8]. The spectra were taken with an excitation energy 647 nm (1.92 eV), which is highly in resonance with the (7,5) SWNT species. The inset of the figure shows a magnified view of a portion of the intermediate frequency mode (IFM) region. All four spectra are normalized with respect to their G-band intensities. (b) Shows the difference spectra between the finite length samples and the as-grown sample in the IFM region. The spectra were calculated by subtracting the spectra of the as-grown sample from the spectra of the three short samples.

Raman spectra, and higher relative IFM intensities (I_{IFM}/I_G) are observed.

To show the effects of nanotube length on the Raman intensities more clearly, we plot in Fig. 1b the difference spectra between the SEC-treated SWNT samples and that of the as-grown sample. Even though most of the IFM frequencies observed are consistent with the mode frequencies reported in previous Raman studies [5,10], with a small frequency variation due to curvature effects, the length dependence of the IFM intensity appears to be different for IFM features arising from different physical origins. The intensities for the near Γ point modes at 838 cm^{-1} and 911 cm^{-1} (near Γ point combination IFM features [5]) do not change much with deceasing L_{tube}. On the other hand, for the 610 cm^{-1} feature associated with the near-M-point symmetry-breaking process [5], the relative Raman intensity is found to increase significantly with decreasing L_{tube}. At the given values of E_{laser}, it is possible to assign 760 cm^{-1} to either a near-M-point feature or to a combination IFM feature, as the counterpart for the observed 911 cm^{-1} combination IFM feature. Compared to the 911 cm^{-1} mode, the 760 cm^{-1} mode has a significantly larger intensity increase with respect to the decrease in the average L_{tube}. This observation suggests that the 760 cm^{-1} feature probably arises from a combination of the two mechanisms, in which the symmetry breaking near-M-point process is responsible for the large intensity increase with decreasing average nanotube length.

In general, the Raman intensities in the IFM region are very low because many of the Raman-active IFM features correspond to long wavelength vibrations along the axial direction.[1] In short nanotubes, the amplitudes for the selected IFM vibrations are expected to be enhanced. Since the exciton-optical matrix element is proportional to $L_{tube}^{1/2}$ [16], the optical intensity per L_{tube} does not depend on L_{tube}. Thus, the L_{tube} dependence should come from the exciton–phonon matrix element [16] or the elastic scattering matrix element, which are not investigated theoretically in the present report. As nanotube-shortening lowers the translational symmetry, more Raman-active features in the IFM region are also expected to appear. Similarly, the reduced symmetry for short nanotubes is also expected to activate the IR-active modes in the Raman spectra, which would otherwise be silent, for the infinite-length SWNT system, in which the sp^2 -bonded carbon network is unlikely to support any static dipole. In the present work, several IR-active modes were consistently observed at 1189 cm^{-1}, 1405 cm^{-1}, and 1460 cm^{-1} for a number of values of E_{laser}. The frequencies for these observed IR modes are consistent with those reported previously [13].

To further investigate the IFM structures of different (n,m) species around the same energy region, the samples were studied at three additional values of E_{laser}, as shown in Fig. 2. For these values of E_{laser}, several species of similar diameter semiconducting SWNTs with different chiral angles contribute significantly to each of the spectra. The common IFM features as well as their possible assignments are summarized in Table 1, and in the caption for Fig. 2.

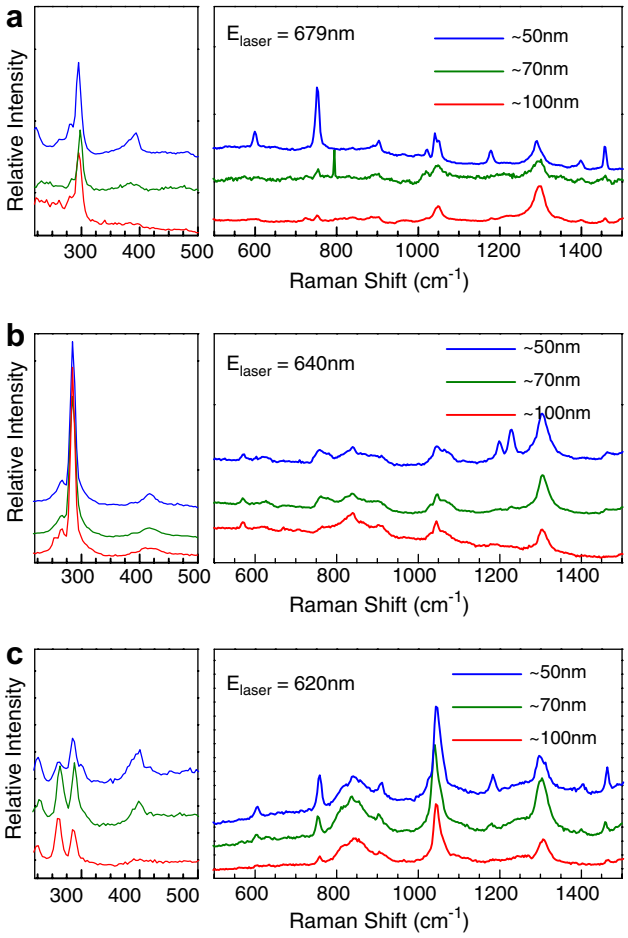

Fig. 2. Resonance Raman spectra in the RBM and IFM region of DNA-wrapped SWNTs with different L_{tube}, taken at (a) $E_{laser} = 679$ nm (1.83 eV), (b)$E_{laser} = 640$ nm (1.94 eV), and (c) $E_{laser} = 620$ nm (2.00 eV). These values of E_{laser} emphasize (a) (8,3), (b) (7,5), and (c) (7,5) and (11,1) semiconducting SWNT species, respectively.

Fig. 3a–c shows the evolution of the relative IFM intensities, in which the increase in the I_{IFM}/I_G ratio relative to its value for $(1/L_{tube}) = 0.010$ is plotted for various tubes as a function of inverse L_{tube} for different values of E_{laser}. As the values of E_{laser} are changed from 647 nm (Fig. 1) to 620 nm, the E_{laser} moved into and out of the resonant window of the (7,5) SWNT ($E_{ii} \sim 642$ nm [14]), and then gradually moved into the resonance window of the (11,1) SWNT ($E_{ii} \sim 606$ nm [14]). Fig. 3b shows a clear pattern of the IFM intensity evolution when the E_{laser} is strongly in resonance with the (7,5) SWNT. For the two non-dispersive Raman features originating from the Γ point at 840 cm^{-1} and 911 cm^{-1}, their intensities do not increase significantly with decreasing length, since the change in length does not affect the out-of-plane and totally symmetric vibrations. These two modes consistently show the weakest dependence on length for all values of E_{laser}. On the other hand, the intensities for the vibrational features related to near-M-point processes at 610 cm^{-1} and

Table 1
IFM features and their frequencies[a]

Raman shift (cm^{-1})	Observed at E_{laser} (nm)	Assignments [5,6,12]	Comments
610	647, 679, 620	oTO/iTA near-M-point	Large initial I_{IFM} increase with decrease L_{tube}
761	647, 679, 640, 620	oTO/iTA near-M-point	Large initial I_{IFM} increase with decrease L_{tube}
761	647, 679, 640, 620	Combination near Γ point IFM	Large initial I_{IFM} increase with decrease L_{tube}
838–842	647, 679, 640, 620	oTO near Γ point	Small length dependence
911	647, 679, 640, 620	Combination near Γ point IFM	Small length dependence
1045–1051	647, 679, 640, 620	Carbonyl vibration	Large continuous I_{IFM} increase with decrease L_{tube}
1189	647, 679, 640, 620	IR and fullerenic	Large continuous I_{IFM} increase with decrease L_{tube}
1234	640, 620 (occasionally)	Possibly IR	Large continuous I_{IFM} increase with decrease L_{tube}
1291–1309	647, 679, 640, 620	D-band	Large continuous I_{IFM} increase with decrease L_{tube}
1403–1410	647, 679, 640, 620	IR and fullerenic	Large continuous I_{IFM} increase with decrease L_{tube}
1460	647, 679, 640, 620	IR and fullerenic	Large continuous I_{IFM} increase with decrease L_{tube}

[a] oTO here denotes out-of-plane transverse optical phonon modes, whereas iTA denotes in-plane transverse acoustic phonon modes.

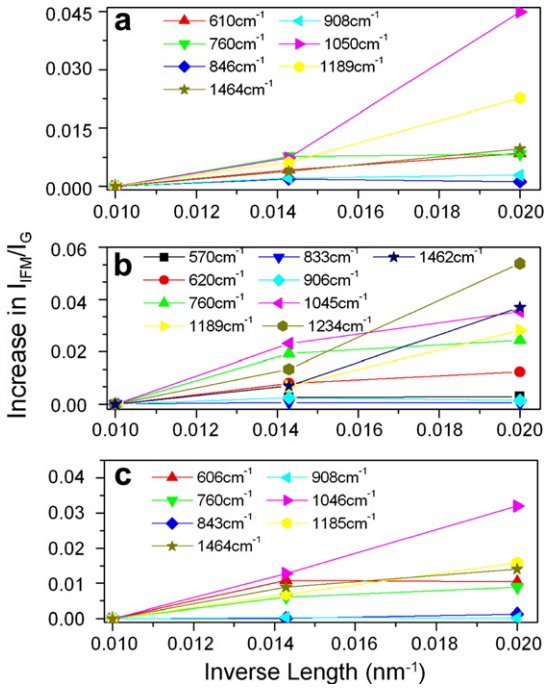

Fig. 3. Evolution of the increase in relative IFM intensity, I_{IFM}/I_G, with respect to the 100 nm sample, plotted as a function of inverse nanotube length ($1/L_{tube}$) for (a) $E_{laser} = 647$ nm, (b) $E_{laser} = 640$ nm, and (c) $E_{laser} = 620$ nm.

760 cm^{-1} show a rapid initial increase in the intensity when the average tube length changed from 100 nm to 70 nm. The rates of the increases slowed down when the average nanotube length changed from 70 nm to 50 nm. Lastly, the intensities for the three modes at 1050 cm^{-1}, 1189 cm^{-1}, 1462 cm^{-1}, increased rapidly without slowing down as the lengths of the nanotubes become short.

As the (7,5) species becomes slightly out of resonance and as more (n,m) species become in resonance with $E_{laser} =$ 647 nm and 620 nm, as shown in Fig. 3a and c, the patterns of the IFM intensity evolution became less clear. With decreasing average L_{tube}, more Raman peaks appear within the same spectral region and often with overlapping spectral intensities as the diameter, chirality, and family dependence become important. In general, Fig. 3a shows mostly similar trends in the IFM intensity (with slightly lower overall intensity) compared to Fig. 3b since both E_{laser} values emphasize the (7,5) SWNT ($E_{laser} = 647$ nm and 640 nm). As more (n,m) species contribute to the spectra, as shown in the case of Fig. 3c, where $E_{laser} = 620$ nm (2 eV), the relative intensities for the near-M-point modes appear to increase at the same rate as the 1000–1200 cm^{-1} modes. Even though the relative intensities for the near Γ point features around 840 cm^{-1} do not change much with L_{tube}, they do appear much broader in the Raman spectra, as seen in Fig. 2c, because more components associated with the different resonant (n,m) species are observed at the corresponding E_{laser}.

The 1050 cm^{-1} Raman feature observed in all of the samples has been previously identified to be a signature of an asymmetric C–O stretch vibration originating from adsorbed CO_2 and contaminants in the sample [10]. This explanation is consistent with the occurrence of the 1050 cm^{-1} peak observed for our sample, since the same transition has been reported to occur at the same frequency for all of the samples regardless of the diameter distributions for SWNTs synthesized using different methods [10]. For all values of the E_{laser} shown in Fig. 3, the relative intensity for this feature shows a large increase with decreasing nanotube length. Since the adsorption events are more likely to occur at the end caps per unit surface area, it is possible that the adsorption events increase as the relative contribution from the end caps increase, which is associated with decreasing nanotube length.

The increased contribution of the nanotube end caps also gives rise to spectral features associated with fullerenes in the IFM region and shows a much larger dependence on L_{tube}. Even though the observed Raman features around 1189 cm^{-1}, 1402 cm^{-1}, and 1462 cm^{-1} correspond to the vibrational energy of previously observed IR features, which will likely be activated by translational symmetry breaking, these vibrational frequencies have also been observed in different fullerenic structures, such as C_{60} and C_{70} [15]. Since the short nanotubes samples emphasize the contribution from the hemispherical end caps, which have a similar geometry and vibrational structure as fullerenes, the large increase in the intensity observed at these

IFM frequencies can probably be partially attributed to contributions from the end caps.

Several IFM features observed in this experiment are not discussed in detail in terms of their L_{tube} dependence because the modes are either too weak or that they do not appear consistently from one spectrum to another. The peak at 1401 cm^{-1} has been observed in many of our data sets and has been identified to be an IR-active mode, a fullerenic vibration, or a combination of both. However, since the peak is very weak, it is difficult to determine its length-dependent behavior. Similarly, the mode around 1234 cm^{-1} has been consistently observed when $E_{laser} = 640$ nm (and sometimes also at 620 nm). Even though the vibrational frequency is close to one of the previously reported IR modes, additional systematic studies will be needed to study and to explain the specificity to the E_{laser} and the large intensity increase that is observed with decreasing L_{tube}.

Even though DNA molecules do give rise to weak vibrational features in the IFM region, the resonantly enhanced Raman modes arising from carbon nanotubes are roughly one order of magnitude higher in intensity in the IFM region. Therefore, the observed increasing IFM intensities (relative to the similarly DNA-wrapped ensemble sample), with IFM frequencies corresponding to previous Raman studies of SWNTs, most likely arise from the intrinsic properties of the carbon nanotubes instead of the DNA molecules.

4. Summary

In this report, a systematic resonance Raman study has been carried out on DNA-wrapped SWNTs as a function of nanotube length, using different values of E_{laser}. As the length of the nanotubes become significantly shorter than the wavelength of light, we have observed a large increase in the Raman and IR mode intensities in the IFM region of the Raman spectra, as a result of the broken translational symmetry in the axial direction. The study has provided direct experimental evidence for finite length effects in the IFM region, predicted in previous bond-polarization calculations [1]. The different pattern of increase in I_{IFM} with respect to $1/L_{tube}$ also provides insights into the different symmetry breaking processes for the individual IFM features originating from different high-symmetry points of the Brillouin zone.

Acknowledgements

MIT authors acknowledge support from NSF grant DMR04-05538 and the Intel Higher Education Program. The work was carried out using the Raman facility in the Spectroscopy Laboratory supported by NSF-CHE 0111370 and NIH-RR02594 Grants. A.J. acknowledges CNPq and the Rede Nacional de Pesquisa em Nanotubes de Carbono, Brazil. R.S. acknowledges a Grant-in-aid (No. 16076201) from Ministry of Education, Japan.

References

[1] R. Saito et al., Phys. Rev. B. 59 (1999) 2388.
[2] A. Rahmani et al., Phys. Rev. B 66 (2002) 125404.
[3] A. Rochefort et al., J. Phys. Chem. B 103 (1999) 641.
[4] L. Alvarez et al., Chem. Phys. Lett. 320 (2000) 441.
[5] C. Fantini et al., Phys. Rev. Lett. 93 (2004) 087401.
[6] C. Fantini et al., Phys. Rev. B. 72 (2005) 085446.
[7] X.Y. Huang et al., Anal. Chem. 77 (2005) 6225.
[8] M. Zheng et al., Nat. Mater. 2 (2003) 338.
[9] M. Zheng et al., Science 302 (2003) 1545.
[10] Z. Ming, B. Diner, J. Am. Chem. Soc. 126 (2004) 15490.
[11] S.G. Chou et al., Appl. Phys. Lett. 90 (2007) 131109.
[12] M.A. Pimenta et al., Phys. Chem. Chem. Phys. 9 (2007) 1.
[13] U.J. Kim et al., Phys. Rev. Lett. 95 (2005) 157402.
[14] S.G. Chou et al., Chem. Phys. Lett. 397 (2004) 296.
[15] M.S. Dresselhaus et al., Science of Fullerenes and Carbon Nanotubes: Their Properties and Applications, Academic Press Inc., 1996.
[16] J. Jiang et al., Phys. Rev. B. 75 (2007) 035405.